Available online at www.sciencedirect.com

SciVerse ScienceDirect

Physics Procedia 41 (2013) 216 – 224

Physics Procedia

Lasers in Manufacturing Conference 2013

Fluid dynamic effects in keyhole welding – an attempt to characterize different regimes

P. Berger*, H. Hügel

Institut für Strahlwerkzeuge (IFSW), Universität Stuttgart, Pfaffenwaldring 43, 70569 Stuttgart, Germany

Abstract

During keyhole welding with lasers a surplus pressure has to act at the keyhole front which drives the molten material around the keyhole. Depending on the travel speed and keyhole diameter, its value can reach several bar and may, therefore, represent a significant contribution to the pressure balance in the keyhole. As a consequence, an effect also on its stability must be expected therefrom. On the basis of simplified, yet physically reasonable estimations, the pressure balance in the keyhole for a wide parameter range of travel speed and keyhole diameter is inspected in detail. By comparing the magnitude of dynamic pressure of the melt flow at the keyhole`s side to the other contributions to keyhole pressure, i. e. ambient pressure and closing pressure due to surface tension, different parameter regimes can be identified where a keyhole with a stable geometry can exist and where not. The theoretical predictions and conclusions agree well with experimental observations of other authors.

Keywords: Laser welding; Keyhole pressure; Keyhole stability; Characteristic welding regimes

1. Introduction

It is common practice to discuss the various mechanisms involved in keyhole welding along with the travel speed. In fact, for given laser power and focusing conditions, with increasing welding speed the appearance of phenomena such as keyhole and weld pool instabilities, spatter formation and humping follows a more or less observable scheme. A systematic experimental investigation of fluid dynamic features and their assignment to

* Corresponding author. Tel.: +49-711-685-66843; fax: +49-711-685-66842.
E-mail address: Peter.Berger@IFSW.Uni-Stuttgart.de.

doi:10.1016/j.phpro.2013.03.072

this parameter is presented in [1]. Such an approach is of interest not only with respect to a better understanding of process mechanisms but also of practical importance since the usable range of welding speed is (apart from possible technical restrictions) generally limited by those events that reduce the quality of the process result. With today`s choice of different laser types, providing high power levels at almost any desired beam quality, the applicable spot diameters range from several tens to some hundreds of micrometer. A characterization of different welding regimes and corresponding features along the lines of [1] with, therefore, taking into account in addition the influence of the spot diameter, could contribute to the comparability of experiments reported by several authors. An attempt to do this is undertaken in this study which is based on a simplified discussion of fundamental facts concerning the pressure balance in the keyhole. In particular, an answer will be sought to the question whether and why the travel speed can dominate the keyhole`s state of geometric stability.

Ever since first diagnostic investigations have shown a complex 3d flow field in the weld pool during keyhole welding [2], the search for the causing mechanisms has been a major topic of research work. Today it is generally agreed that the following "driving forces" contribute to the momentum balance of the melt:

(1) The flow around (and partly beneath) the keyhole driven by the recoil pressure of evaporation at the front,
(2) Pressure forces acting on moving steps at the keyhole front producing there a melt flow component parallel to the laser beam axis,
(3) Friction and direct impact effects of vapor/plasma flow(s) and
(4) Temperature dependent surface tension, e.g. [3] to [9] to list but a few relevant publications.
(5) In addition, welds in ice have revealed a mechanism which, so far, has not been considered, i.e. the collapse of parts of the keyhole and/or cavities which, as a consequence of condensation, induces a strong flow with components towards the keyhole front and to its tip resulting in eddies in the lower part of the pool [10]. Recently, this effect was also seen in simulations of keyhole welding of steel [11] which can be taken as indication that it occurs in a real process as well. Investigations of keyhole behavior in liquid zinc have led to the conclusion that condensation of metal vapor would be responsible for the entrainment of shielding gas into the keyhole [12], which also gives evidence of this phenomenon.

Since the flow around the keyhole is that phenomenon with the most obvious and direct linking to the travel speed, it appears reasonable trying to characterize speed dependent process features along this parameter.

2. Pressure balance in keyhole

In theoretical treatments of keyhole phenomena the pressure inside a keyhole, p_k, is generally considered as the quantity counterbalancing the closing pressure due to surface tension, p_s. For a cylindrical keyhole with a diameter d_f, also assumed here, the closing pressure is given by

$$p_s = 2\gamma / d_f . \qquad (1)$$

The value defined by Equ. (1), however, merely represents an overpressure above the ambient pressure p_∞. The pressure inside the keyhole then should read

$$p_k = p_\infty + p_s . \qquad (2)$$

If it is assumed that no ambient gas is present in the keyhole, p_k is equal to the vapor pressure p_v therein, which has to be established by an adequate evaporation rate at the keyhole wall. For this, instead of considering the energy balance, a temperature distribution at the wall is presumed such that $p_v = f(T_v)$ yields

the necessary value of p_v. Further assumptions resp. simplifications in the course of these investigations are that the hydrostatic pressure and any vapor flow components in the keyhole are neglected. Thus, only phenomena will be considered that occur in a plane normal to the laser beam axis and parallel to the work piece`s surface.

With this laying-down, the pressure along the circumference and over the cross section of the keyhole is constant as long as there is no traverse movement, $v = 0$, see Fig.1 (left). However, even for the case of $v = 0$, any geometric deviation from axial symmetry, for example with elongated cross sections with varying curvature, as shown also in Fig.1 (center and right), leads to a variation of p_s along the wall. Of course, this is inconsistent with the idea or assumption of a homogeneous pressure – a contradiction that could be resolved by allowing for a flow field of gas (vapor, plasma, ambient and/or shielding gas) in the keyhole.

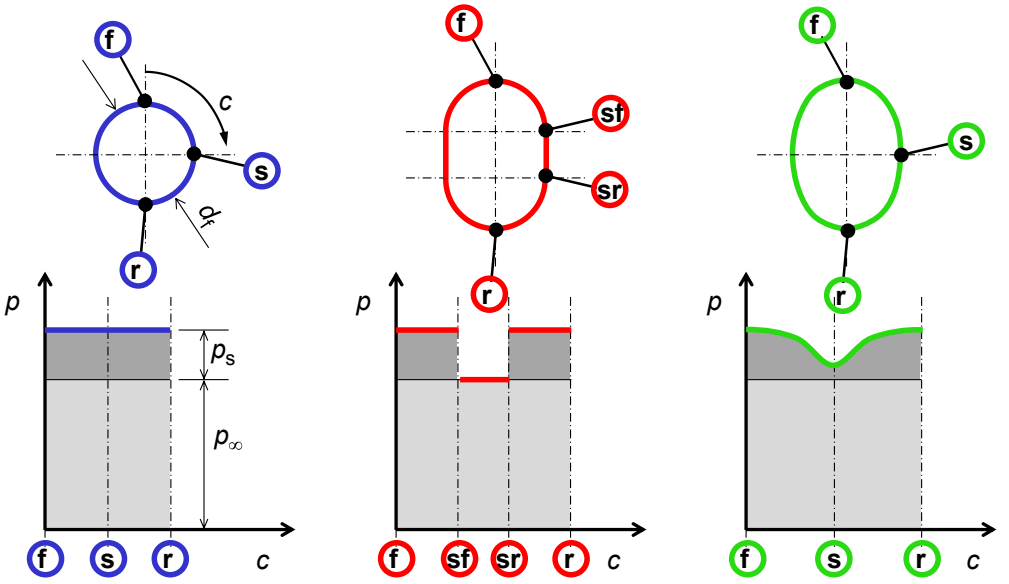

Fig. 1. Ambient pressure p_∞ and closing pressure p_s (inversely proportional to the local curvature) along the circumference of a keyhole with cylindrical (left) and elongated (right) cross sections.

When the keyhole is moved through the work piece with a traverse speed v, an additional amount of pressure is needed at the front to produce the melt flow around it. Since high speed values shall be considered herein as well, their effect on the pressure balance must not be neglected. Therefore, the maximum melt velocity at the keyhole`s side and the corresponding pressure drop Δp which the flow is experiencing during its acceleration shall be calculated as functions of v and d_f.

The anticipated situation is discussed along Fig. 2: At left, the front part of the weld pool and the keyhole, that is assumed to retain its circular cross section, are shown together with the path of a volume element travelling relative to the keyhole (kept fixed in space) from position “m” to “p”; the pressure histogram is qualitatively depicted on the right. Starting with a velocity equal to the welding speed v it is decelerated to zero at the keyhole front “f” attaining there the stagnation pressure $p_0 = \rho v^2/2$. Then it is accelerated to the maximum value u_m at the side “s”; according to Bernoulli’s equation (describing momentum conservation in a stationary, non viscid stream line) this is related to a pressure drop Δp from “f” to “s”. At this point it has to be emphasized that the absolute pressure level at “s” is not known. Nevertheless, it appears reasonable to

assume the static pressure there to be $p_k = p_s + p_\infty$ (above that, with regard to the effect to be discussed, it is the pressure difference Δp rather than the absolute value that counts). Following the streamline further, potential flow theory would predict at the rear stagnation point "r" the same value as at the front. However, due to viscous effects it should be lower what is indicated by the dashed pressure course (according to [3] it reaches only about 20 to 40%). - In any case, a flow around the keyhole results in a varying pressure at its wall and contradicts the assumption of a homogeneous constant pressure. Again, as for non circular cross sections at $v = 0$, this could be resolved by allowing for some flow field in the keyhole.

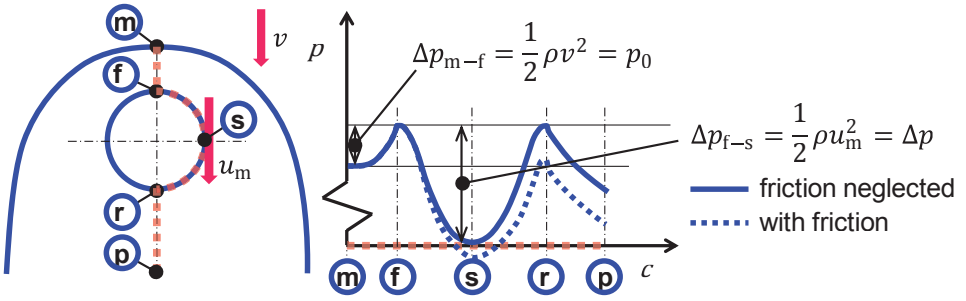

Fig. 2. Qualitative pressure distribution along a streamline starting from melting of a volume element at the solid/liquid boundary at "m" and ending in the weld pool somewhere behind the keyhole at "p"; see text.

Numerical studies of melt flow in the weld pool in [3], [4], [13], [14] show that the melt velocity at the side walls of a cylindrical keyhole can amount up to values more than an order of magnitude higher as the travel speed, and the corresponding dynamic pressures may reach 10 bar and more [15]. To straightforward demonstrate the effects of both parameters, travel speed v and keyhole diameter d_f, a simplified approach is used here for obtaining those figures. It follows the results of a model based on heat conduction which yields the weld pool geometry. From its width and by assuming a linear velocity distribution reaching from $u = v$ at the pool edge to a maximum value u_m at the keyhole side, conservation of mass leads to an analytical approximation given in [15] which is used here:

$$u_m = v\,(1 + c \cdot Pe^{3/4}). \tag{3}$$

In this expression for the maximum velocity the term c contains material properties and Pe denotes the Péclet number defined as $Pe = v\,d_f / k$; k is the heat diffusivity. The corresponding dynamic pressure $\rho\,u_m^2/2$, which is equal to the pressure drop from "f" to "s" in Fig. 2, then can be expressed as a function of v and d_f:

$$\Delta p = \rho v^2/2\,(1 + c \cdot k^{-3/4}\, v^{3/4}\, d_f^{3/4})^2. \tag{4}$$

The results of calculations for a wide range of parameters v and d_f are plotted in Fig. 3 and reveal some interesting features: If the second terms in the parantheses of equations (3) and (4) are small compared to 1, it follows that the melt velocity is not much higher than the welding speed and the dynamic pressure Δp can be approximated by the stagnation pressure p_0. In general, this is a small value compared to p_∞ or p_s. However, approaching large Péclet numbers, i.e. large values of v and d_f, Δp comes to a proportionality close to $\Delta p \sim v^{3,5}$ and $d_f^{1,5}$, which also is indicated in Fig.3. Important to note are the facts that for such parameters the dependence of Δp on d_f can no longer be ignored and the considerable high values of Δp have to be considered in the momentum balance of the keyhole.

It becomes evident from the sketch in Fig. 2 and the numbers of Δp in Fig. 3 that with increasing travel speed (and keyhole diameter) an axial symmetry (being representative for a homogeneous pressure in the keyhole) will be destroyed more and more due to an increasing need of evaporation and rising pressure at the front. It therefore suggests itself to consider the magnitude of the dynamic pressure Δp compared to that of the other contributions to the keyhole pressure as a measure for the deviation from the condition of axisymmetric equilibrium and expected consequences resulting therefrom.

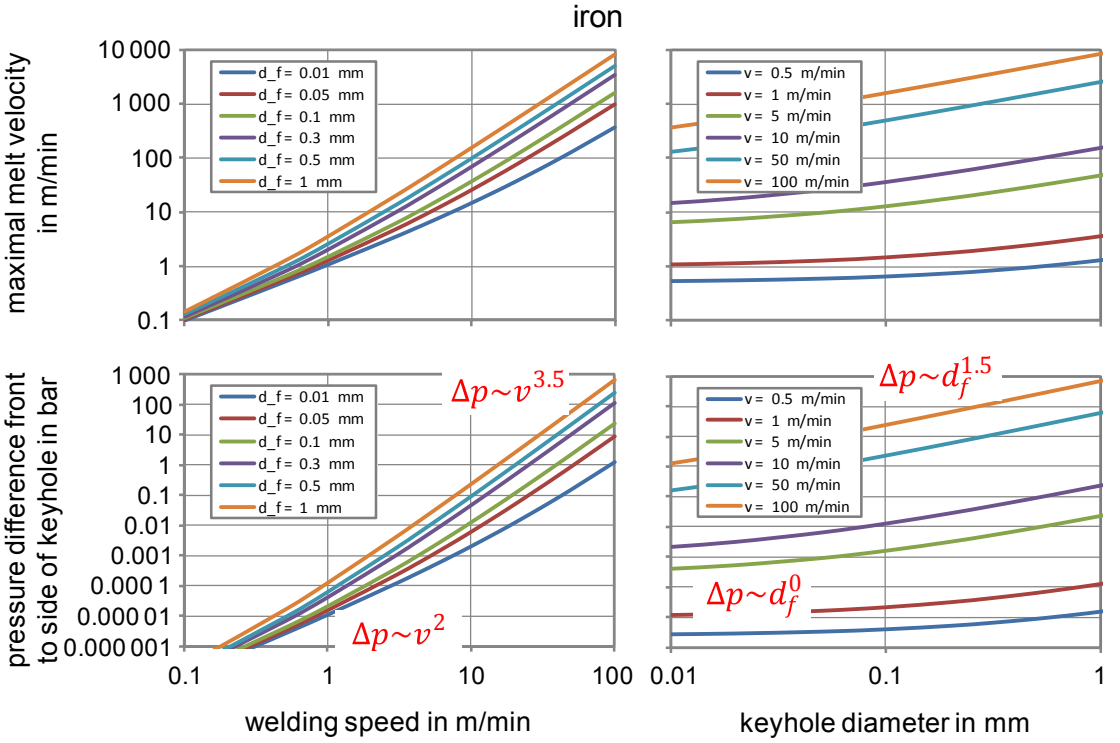

Fig. 3. Analytically calculated maximum melt velocity at the side wall of cylindrical keyholes with diameter d_f and corresponding dynamic pressure in dependence of welding speed and keyhole diameter.

In doing this, values of p_s, p_k and Δp are plotted as function of d_f in Fig. 4, where the influence of v is expressed parametrically by the curves $\Delta p(v)$. Several aspects shall be pointed at further:

- At very small diameters, p_k is dominated by the closing pressure p_s.
- At large keyhole diameters, the keyhole pressure is determined by the ambient pressure because p_s is of minor importance here.
- Since, for a given travel speed, Δp increases with d_f the influence of flow around the keyhole will be more pronounced at higher d_f which means that here already at lower values of v a deviation from axisymmetric equilibrium conditions will occur.
- At larger diameters, therefore, a reduction of ambient pressure will enhance the effect of Δp.
- For each value of d_f, it is possible to distinguish between different regimes according to the relative magnitude of Δp, p_k resp. p_s, what is being done next.

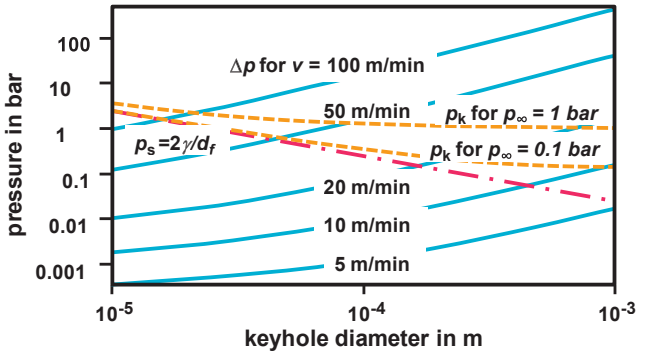

Fig. 4. Dynamic pressure Δp, closing pressure p_s and keyhole pressure p_k according to Equ.(2) for $p_\infty = 0.1$ and 1 bar in dependence of keyhole diameter. Comparing the magnitudes of these contributions to the pressure balance allows to define parameter regimes where different features are to be expected.

3. Characterization of different regimes

First, in Fig. 5 exemplary are shown the values of the various contributions to the pressure in the keyhole for two extreme situations. On its left side, the parameters v and d_f yield such a small value of Δp compared to p_∞ and p_s, so that its effect on the momentum balance is negligible and the assumption of a circular cross section might still be valid. On the right side, a case is illustrated where the dynamic contribution Δp exceeds the others, in particular p_s. The not drawn pressure increase from "s" to "r" shall indicate that the closing pressure no longer can withstand the dynamic pressure and a keyhole in its real sense cannot exist, it is degenerated to an energy absorbing front.

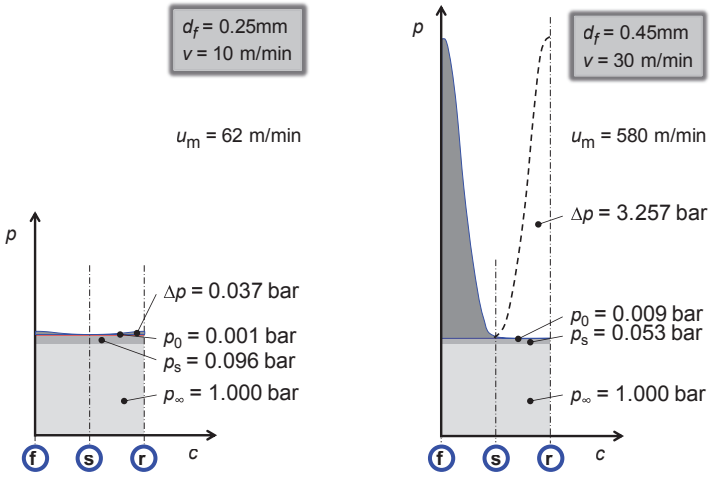

Fig. 5. Drawn to scale contributions to pressure balance for two "extreme" conditions, see text.

However, regarding geometry, both situations may be characteristic for stable conditions since the "disturbing" effect of Δp is either negligible low or the dominating mechanism. By such considerations, in

addition to the two already defined regimes, a third one can be identified what is sketched in Fig. 6. Here, when the dynamic pressure is of the same order of magnitude as the closing pressure, their respective effects – pushing the rear keyhole wall downstream, on the one hand, and trying to retain a circular form, on the other hand – might result in some quasi-steady geometry.

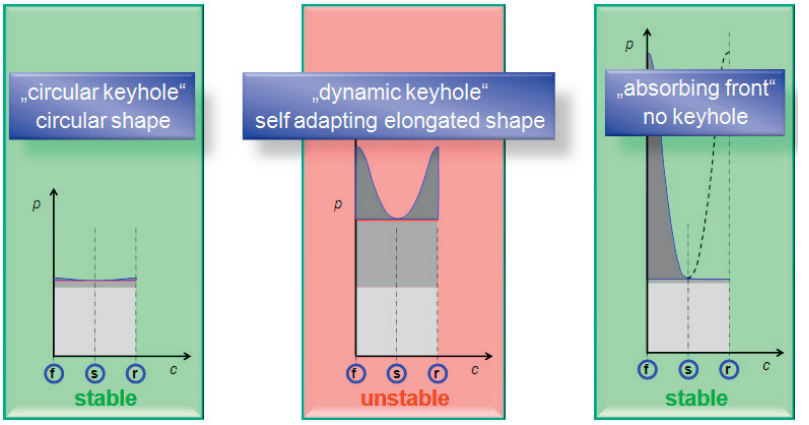

Fig. 6. By comparing the relative magnitude of Δp with that of the other contributions different parameter regimes with respect to the stability of keyhole geometry can be identified.

In the following, some features in the above defined regimes which can be expected and related to real situations during welding experiments shall be discussed along Fig. 7. The graph compares calculated pressure values with those that were deduced from welding speed data characterizing different keyhole geometries [1], [16], [17], [18].

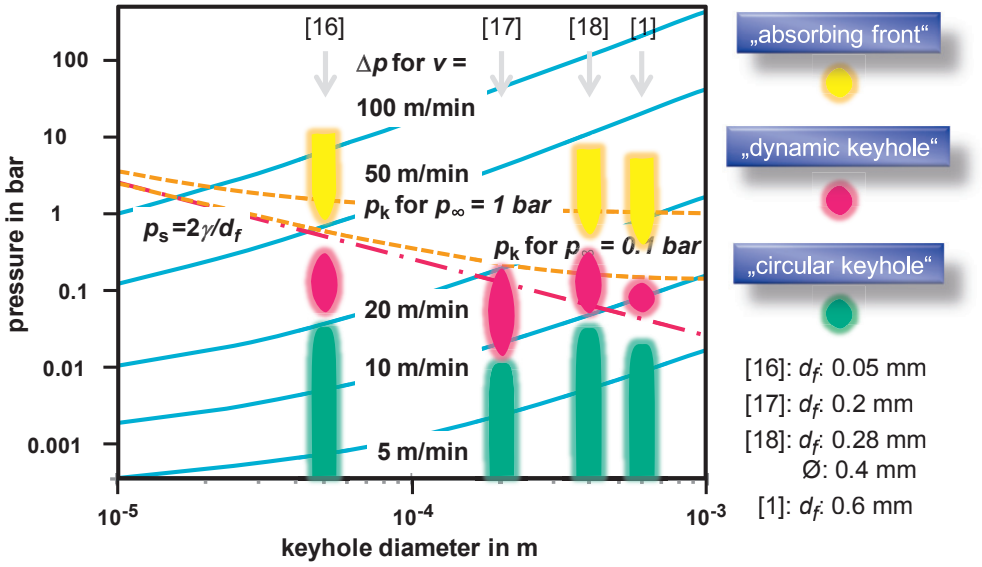

Fig. 7. The experimentally observed features of keyhole geometry and the calculated values of Δp for the corresponding welding speeds and diameters in [1], [16], [17] and [18] agree well with the predictions of the analysis.

3.1. "Thermally determined regime" $\Delta p \ll p_k$

Here, with but low dynamic pressure compared to p_k only a weak deviation from a homogeneous pressure distribution will occur which is the condition for a geometrically stable cylindrical keyhole. The process then is governed by a more or less axisymmetric energy coupling with multiple reflections on the keyhole wall and heat transport by conduction within the weld pool. Its geometry, therefore, can be calculated by "thermal" models, the reason why this regime in [1] is called "Rosenthal" regime. Momentum transfer to the melt predominantly occurs by friction between a mainly axially directed vapor/plasma flow and the keyhole wall; in keyholes with extremely small diameters this can cause a strong flow in the surrounding melt against the laser beam direction with drastic effects on the pool geometry around the keyhole [18]. Experiments in this regime with spot diameters of 0.05 mm [16], 0.2 mm [17], 0.28/0.4 mm [18] and 0.6 mm [1] all show a circular keyhole opening. In addition, X-ray photography in [18] reveals a straight and slender keyhole with no discernible inclination.

3.2. "Front pressure determined regime" $\Delta p \gg p_s$

Under these conditions the closing pressure p_s no longer can counterbalance the dynamic pressure at the rear of the keyhole which is somewhat below yet of the same order as p_0. As a consequence, a capillary which is enclosed by melt cannot exist. The keyhole has evolved to just an inclined front where energy coupling occurs. The downstream distance where the melt streams from the sides (and below) the front merge is determined by geometry dependent cooling [2], [20]. The vapor flow emanating from the front does not interact with the melt behind it, this feature is described in [1] and [16]. Whereas the front is seen to be absolutely stable, humping develops in the melt downstream of the front (however, as pointed out in [20], humping has to be regarded as an instability of melt flow and not of the keyhole).

3.3. "Dynamically determined regime" $\Delta p \approx p_k$

In this parameter range all the experiments [1], [16], [17] and [18] show an elongated keyhole opening and a waviness of the pool. In addition, strong fluctuations of its rear are detected by high speed photography in [18]. The elongation is explained as being caused by the impact of the vapor flow coming from the keyhole front. The dynamic pressures calculated from the experimental welding speed data in the order of 0.1 bar lie close to the values of p_s in the parameter range of cited keyhole resp. spot diameters. Here, the rear keyhole wall is practically not hit by direct radiation and, therefore, not stabilized by the recoil pressure of a noticeable evaporation. On the other hand, some closing pressure is still acting there which causes the wall to find a new position. Since this self-adapting process needs a finite time, the keyhole geometry will exist in a dynamic state with its geometry oscillating around a quasi-steady state.

The herein presented theoretical investigations do not allow drawing direct conclusions with respect to fluid dynamic phenomena such as e.g. spattering. Nevertheless, the good agreement between their predictions concerning keyhole geometry and experimentally observed phenomena in the corresponding parameter regimes encourages adding a few statements to this phenomenon as well. The commonly discussed idea that the in the thermally dominated regime observed small spatters emanating from the keyhole`s rim are predominantly due to frictional effects is supported. The fact, that in the case of an absorbing front no spatter is observed at all is also in agreement with the findings herein. Finally, the interpretation for the heavy spattering appearing in the dynamic regime given e.g. in [10], [17], [18] corresponds well with the herein postulated interaction of dynamic and closing pressure at the keyhole`s rear.

4. Conclusion

The influence of fluid dynamic pressure resulting from the flow around the keyhole has been considered in detail and some conclusions concerning stability of the keyhole geometry could be drawn. In this respect, three different regimes were identified, two of them favoring conditions for stable behavior. In general, however, a stable keyhole geometry cannot exist because of the asymmetrically acting dynamic pressure which depends on traverse speed and keyhole diameter. Experimental observations of keyhole behavior fit well to the identified parameter regimes.

References

[1] Fabbro, R., Slimani, S., 2007. Melt pool dynamics during deep penetration cw Nd:YAG welding, Proc. LIM 2007, p. 259.
[2] Arata, Y., 1986. Plasma. Electron and laser beam technology – development and use in material processing, ASM Int., p.641.
[3] Beck, M., Berger, P., Dausinger, F., Hügel, H., 1990. Aspects of keyhole/melt interaction in high speed laser welding, SPIE 1397, p. 769.
[4] Mahrle, A., Schmidt, J., 2002. The influence of fluid flow phenomena on the laser beam welding process, Int. J. Heat and Fluid Flow 23, p. 288.
[5] Matsunawa, A., Semak, V., 1992. The simulation of front wall dynamics during laser welding, J. Phys. D: Appl. Phys. 30, p. 798.
[6] Matsunawa, A., Kim, J.-D., Katayama, S., Semak, V.V., 1996. Experimental and theoretical studies on keyhole dynamics in laser welding, Proc. ICALEO 1996, Sec. 5, p. 58.
[7] Golubev, V.S., 2003. Laser welding and cutting: recent insights into fluid-dynamic mechanisms, SPIE 5121, p. 1.
[8] Lambrakos, S.G., Metzbower, E.A, Moore, P.G., Dunn, J.H., Monis, A., 1993. A numerical model for deep penetration welding processes, J. Mat. Eng. and Performance. 2, H. 6, p. 819.
[9] Fuhrich, Th., Berger, P., Hügel, H., 2002. Numerical calculation of the weld pool in deep penetration laser welding, Math. Modeling of Weld Phenomena 6, p. 93.
[10] Berger, P., Hügel, H., Graf, Th., 2011. Understanding pore formation in laser beam welding, LIM 2011, Physics Procedia 12, p. 241.
[11] Otto. A., 2013. Modeling of laser beam welding – latest results, 15th Int. Workshop on Process Fundamentals of Laser Welding and Cutting, Hirschegg 2013, Conference CD.
[12] Kaplan, A., Mizutani, M., Katayama, S., Matsunawa, A., 2002. Unbounded keyhole collapse and bubble formation during pulsed laser interaction with liquid zinc, J. Phys. D: Appl. Phys. 35, p. 1218.
[13] Aalderink, B.J., de Lange, D.F., Aarts, R.G.K.M., Meijer, J., 2006. Experimental verification of multi-physical modeling of the keyhole welding process, Proc. ICALEO 2006, p. 479.
[14] Schuster, R., 2008. Melt bath shapes and keyhole vapor pressure, in: Math. Modeling of Material Processing with Lasers 2008, Igls/Innsbruck.
[15] Beck, M., 1996. Modellierung des Lasertiefschweißens, PhD - thesis, Univ. Stuttgart, B.G. Teubner, Stuttgart.
[16] Hess, A., Dausinger, F., 2008. Humping mechanisms during high-speed welding with brilliant lasers, PICALO 2008, Proc. CD, paper #8.
[17] Weberpals, J.-Ph., 2010. Nutzen und Grenzen starker Fokussierung beim Laserschweißen, PhD-thesis, Univ. Stuttgart, Herbert Utz Verlag.
[18] Rominger, V., Harrer, Th., Keßler, St., Braun, H., Dorsch, F., Abt, F., Jarwitz, M., Heider, A., Weber, R., Graf, Th., 2012. Formation mechanisms of process instabilities and strategies to improve welding quality, ICALEO 2012, paper #1709.
[19] Kittel, S., 2011. Private communication on „vulcano effect“ in context with ”Verzugsarmes Laserstrahlschweißen an axialsymmetrischen Bauteilen“, PhD - thesis, Univ. Stuttgart, Herbert Utz Verlag 2011.
[20] Berger, P., Hügel, H., Hess, A., Weber, R., Graf, Th., 2011. Understanding of humping based on conservation of volume flow, LIM 2011, Physics Procedia 12, p. 232.